https://doi.org/10.33472/AFJBS.6.9.2024.2444-2458

African Journal of Biological Sciences

Journal homepage: http://www.afjbs.com

Research Paper Open Access

Modeling the synthesis and kinetics of Ferrous Sulfate production: Towards Sustainable Manufacturing Processes

Sanjeev Kumar[1], Suraj Mandal[2], Neha Priya[3], Farah Deeba[4], Vinay Hiralal Singh[5], Gajanan Chandrakant Upadhye[6], Anupama Rawat[7], Mamatha Devi A.B[8], Rohit Tomer[9]*

[1]Research Scholar, Academy of Scientific and Innovative Research (AcSIR)

[2]Assistant Professor, Department of Pharmacy, IIMT College of Medical Sciences, IIMT University, O-Pocket, Ganganagar, Meerut, 250001, U.P., India

[3]Assistant Professor, IIMT College of Pharmacy, Greater Noida, U.P., India

[4]Assistant Professor, Sharda university

[5,6]Assistant Professor, Konkan Gyanpeeth Karjat College of ASC Karjat Raigad Maharashtra 410201

[7]Assistant Professor, Graphic Era Hill University Clement Town Dehradun Uttarakhand Pincode 248001

[8]Assistant Professor of Chemistry, Maharani's science college for women (Autonomous),J.L.B Road, Mysoe-570005

[9]Dental Surgeon AND Public Health Specialist, Academy of Scientific & Innovative Research (AcSIR)

Corresponding Author Details:

Rohit Tomer, Dental Surgeon AND Public Health Specialist, Academy of Scientific & Innovative Research (AcSIR)

Email: rohitotomar1116@gmail.com

Volume 6, Issue 9, 2024

Received: 27 Feb 2024

Accepted: 28 Mar 2024

doi: 10.33472/AFJBS.6.9.2024.2444-2458

Abstract:

This Research provides a thorough summary of modeling attempts to comprehend the chemistry and kinetics of ferrous sulfate production, with an emphasis on developing sustainable manufacturing techniques. One efficient way to clean wastewater containing dyes is through chemical oxidation. The most potent and environmentally benign oxidant for aqueous media is ferrate. The goal of this work is to use ferrate, which is made from the ferrous ion of FeSO4.7H2O via a wet chemical process, to breakdown Remazol Black B colors. This study analyzes the adequacy of ferrate to permanganate, peroxide, and dichromate in debasing Remazol Black B colors. It additionally looks at the best debasement conditions, like pH, molar proportion, and ideal time, as well as the kinetics of corruption. Emazol black B can be productively oxidized by ferrate at an optimal pH of 8, a molar proportion of ferrates to colors of 5:1, an optimal corruption term of 120 minutes, and a debasement level of up to 95%, as per the outcomes. The reason for this work is to reveal insight into the principal components that control the combination and kinetics of ferrous sulfate to work on the productivity and maintainability of modern activities in the compound assembling industry.

Keywords: *Kinetics, Ferrous, Sulfate, Emazol Black, Oxidation*

1. INTRODUCTION

The necessity of sustainability has become a driving principle in today's industrial landscapes, directing research and development efforts toward resource- and eco-efficient production processes [1]. The chemical industry is one of the many sectors looking for sustainable solutions because its complex synthesis processes can result in major environmental consequences [2]. In this regard, the production of ferrous sulfate, an ingredient essential for a number of industrial uses, from agriculture to water treatment, captures the potential and difficulties of sustainable manufacturing [3]. A basic chemical compound with a broad range of commercial uses is ferrous sulfate (FeSO4) [4]. Its importance stems from both its use as an economical nutrient supplement in farming operations and its critical function in water treatment, where it eliminates pollutants such as hydrogen sulfide and phosphates [5]. Ferrous sulfate is also used in the manufacturing of medications, iron pigments, and chemical reactions such cement chromate reduction [6]. The optimization of ferrous sulfate production processes has significant promise for improving sustainability across different sectors due to its varied application [7]. The oxidation of iron or the dissolving of iron-containing materials in sulfuric acid are two examples of energy-intensive and environmentally harmful processes used in traditional ferrous sulfate production methods [8]. These traditional methods contribute to resource depletion and environmental damage by using a lot of energy and producing a lot of trash and pollutants [9]. To address these issues and lessen the environmental impact of ferrous sulfate production, scientists and industry professionals are increasingly focusing on creative and sustainable manufacturing methods [10].

The modeling of ferrous sulfate production syntheses and kinetics is an essential first step toward the realization of sustainable manufacturing processes in this field [11]. Through the application of computational modeling and kinetic analysis, scientists can obtain significant understanding of the fundamental processes that regulate the synthesis of ferrous sulfate [12]. With this information, reaction conditions, catalysts, and process parameters can be optimized to increase productivity, decrease waste, and have a minimal negative impact on the environment [13]. Furthermore, the production of ferrous sulfate sustainably has the capacity to trigger more significant changes in the chemical sector [14]. Developments in ferrous sulfate synthesis might spur similar breakthroughs in other chemical processes and serve as a model for environmentally friendly manufacturing methods, leading to a paradigm shift towards sustainability in the industry [15]. Furthermore, in a world where resources are becoming scarcer, the advancement of sustainable manufacturing technology boosts industry resilience and competitiveness while also helping the environment [16]. This research attempts to investigate the synthesis and kinetics of ferrous sulfate production via a sustainability lens in light of these factors [17]. This work aims to add to the continuing discussion on sustainable manufacturing processes by analyzing the state-of-the-art in ferrous sulfate synthesis, clarifying the main obstacles and opportunities, and suggesting novel modeling strategies [18]. It is our shared goal to clear the path for a more sustainable future in which chemical synthesis complies with the values of resource conservation and environmental stewardship via interdisciplinary cooperation and coordinated research efforts.

1.1 Significance of Ferrous Sulfate

Ferrous sulfate (FeSO4) is a fundamental component of industrial chemistry that affects a wide range of applications. Its widespread use highlights its crucial function in tackling a range of pressing issues, including water treatment, pigment manufacture, pharmaceuticals, and different chemical processes [19]. Its importance stems not only from its adaptability but also from its necessity in addressing urgent issues including nutrient replenishment, impurity elimination, and chemical synthesis facilitation. It is beneficial as a nutritional supplement to increase agricultural yields and as an affordable way to remove impurities from water. It helps to create important chemicals in the manufacturing of pigments and pharmaceuticals, and it is an important catalyst or reactant in chemical processes. Thus, ferrous sulfate's diverse range of applications highlights its significance as a cornerstone in a number of industrial sectors and emphasizes the necessity of sustainable manufacturing procedures to guarantee its efficacy and availability going forward.

1.2 Challenges in Conventional Production Methods

Iron oxidation or dissolving in sulfuric acid are two energy-intensive processes that have long been a feature of conventional ferrous sulfate production methods. Although these methods are efficient in producing ferrous sulfate, they have a negative impact on the environment. These operations produce a large amount of trash and emissions, which worsen resource depletion and significantly contribute to environmental damage [20]. The chemical sector urgently needs to accept more sustainable manufacturing processes due to the cumulative environmental impact of such old production methods. Reducing the environmental impact of industrial operations is becoming more and more important as worries about pollution, climate change, and resource scarcity grow. Given this, switching to sustainable production processes for ferrous sulfate presents both a need and an opportunity to encourage environmental responsibility and long-term sustainability in the chemical industry.

2. EXPERIMENTAL SECTION

2.1 Materials

Glass wool, potassium hydroxide (KOH), sodium hypochlorite (NaOCl), hydrogen peroxide (H2O2), potassium permanganate (KMnO4), potassium dichromate (K2Cr2O7), disodium phosphate (Na2HPO4), monosodium phosphate (NaH2PO4), and ferrous sulfate pentahydrate (FeSO4.7H2O) were acquired from Merck. Black B Remazol Aqueous dye with a composition of at least 50% was acquired from Sigma Aldrich, and Diponegoro University Integrated Laboratory was the supplier of dye. Every chemical was utilized without any additional purification.

2.2 Equipment’s

Common glassware, magnetic stirrers (Venjoyit), pH meters, UVVis spectrophotometers (T60UV-Visible Spectrophotometer), analytical balances (O'haus PA214), and chemical oxygen demand (Hach 21525925) are among the tools used.

2.3 Ferrate synthesis from FeSO4.7H2O

Ferrate (FeO4-2) was synthesized by reacting 31 g of KOH with 60 mL of NaOCl solution. Once homogenous, the mixture was agitated further. The solution was then constantly agitated for 30 minutes until it turned a deep purple color after adding 4 g of FeSO4.7H2O.

After a day of standing, the synthesis product was filtered through glass wool. The maximum wavelength of the solution was then determined using a 400–700 nm UV–Vis

spectrophotometer. The concentrations of the synthesized ferrate were also ascertained by measuring the maximum wavelengths.

2.4 Stability test of ferrate solutions

Using a UV-Vis spectrophotometer, the absorbance of the ferrate solution was determined over a period of ten days at the maximum ferrate wavelength. Using Lambert-Beer Law, the resulting absorbance value was transformed to a concentration value.

2.5 Finding the ideal pH degradation

First, a 5:1 ferrate to Remazol Black B ratio was created in order to ascertain the ideal pH of degradation. Using buffer solutions—sodium hydrogen orthophosphate and sodium dihydrogen orthophosphate for pH 7 and 8 and sodium hydrogen orthophosphate, sodium tetraborate, and sodium hydroxide for pH 9–11—the pH of each solution was changed from 7 to 11. Next, 4 mL of each solution was taken, allowed to react for 60 minutes, and the sample's absorbance was measured at Remazol Black B's maximum wavelength.

2.6 Finding the ideal molar ratio for deterioration

By creating molar ratio ferrate: Remazol Black B of 1:1; 2:1; 3:1; 4:1; and 5:1, the molar ratio was determined. By adding a buffer, each sample with a distinct ratio was brought to the ideal pH. The colors and 4 mL of ferrate solution were then combined, and the mixture was agitated for 60 minutes. Remazol Black B's maximum wavelength was measured with a UV-Vis spectrophotometer to determine the solution's absorbance.

2.7 figuring out the ideal moment for degradation

Making a solution of ferrate and Remazol Black B dyes at the ideal pH and molar ratios allowed for the determination of the ideal degradation time. Up to 4 milliliters of each solution were taken, and they were then mixed. Using a UV-Vis spectrophotometer set to remazol black B's maximum wavelength, the absorbance was measured every 10 minutes until 180 minutes had passed.

2.8 Remazol Black B dye degradation and degradation kinetics

The absorbance of the degradation solution was measured at the dye's maximum wavelength using a UV-Vis spectrophotometer. To determine the value of the remazol Black B concentration from degradation, the sample's absorbance value was plotted in the equation produced by a standard curve. Using a UV-Vis spectrophotometer, the degradation solution's wavelengths in the 200–800 nm region were also measured. The following formula was used to determine the percentage of degradation of Remazol Black B dyes:

$$\%\ \text{Degraded Dyes} = \frac{[\text{RBB}]_i - [\text{RBB}]_f}{[\text{RBB}]_i} \times 100\%$$

where [RBB]i denotes the remazol black B concentration at the beginning of the reaction and [RBB]f the concentration at the end of the reaction.

2.9 Comparing KMnO4, H2O2, and K2Cr2O7 with ferrate to see whether one degrades dye more effectively

Solutions with the ideal pH and molar ratio of ferrate degradation were made. Subsequently, four milliliters of each solution were taken and reacted with four milliliters of Remazol black B solution at the optimal ferrate degradation time. Remazol Black B's maximum wavelength was measured with a UV-Vis spectrophotometer to ascertain the absorbance.

2.10 COD analysis

The homogeneity of the sample was the first stage in determining the COD. After that, a digestion solution was applied to a few pipetted samples. Moreover, the solution was maintained at 150 o C ± 2 o C for two hours with closed reflux. At wavelengths of 600 nm or 420 nm, absorbance measurements were performed after the solution had cooled. Next, using the linear regression equation was developed on the calibration curve, the COD content was determined (SNI 6989.2: 2009).

3. RESULT AND DISCUSSION

3.1 Ferrate synthesis

In this work, FeSO4.7H2O and NaOCl were reacted under strong base conditions to create ferrate solution by the wet method. KOH was added to the solution to make it alkaline as ferrate is more stable in an alkaline environment than an acidic one. In an alkaline atmosphere, ferrate species develop, whereas HFeO4 - ion is the dominating species in an acidic atmosphere. FeSO4.7H2O is used in this synthesis as a source of iron (II), while NaOCl is used as an oxidant to convert Fe(II) to Fe(VI). The color of the synthesized ferrate is a particular shade of blackish-purple. This shift in hue denotes the successful synthesis of ferrate, and the total reaction of ferrate synthesis is represented by the following equation:

$$FeSO_4.7H_2O + 2OCl^- + 4OH^- \rightarrow FeO_4^{2-} + 2Cl^- + SO_4^{2-} + 9H_2O$$

3.2 Finding the maximum wavelength of ferrate

The combination's ferrate arrangement has a purple-black tint. Consequently, the greatest frequency of 510 nm can be gotten by describing this arrangement with an UV-Vis spectrophotometer. Ferrate has a frequency retention somewhere in the range of 505 and 510 nm, which is in accordance with the outcomes. The absorbance worth of the ferrate arrangement, which is utilized to decide the centralization of ferrate arrangement, is gotten utilizing this most extreme frequency. Ferrate has a molar absorbance of 1150±25 M-1cm-1 in arrangement at a greatest frequency of 510 nm. The Lambert-Beer Law equation is used to determine the ferrate concentration based on this value.

Table 1: The ferrate solution's absorbance at 400–700 nm in wavelength

Wavelength (nm)	Absorbance
125	0.5
156	0.8
172	0.4
201	0.6
236	0.7
265	0.8
312	0.1
356	0.6
414	0.2
422	0.3

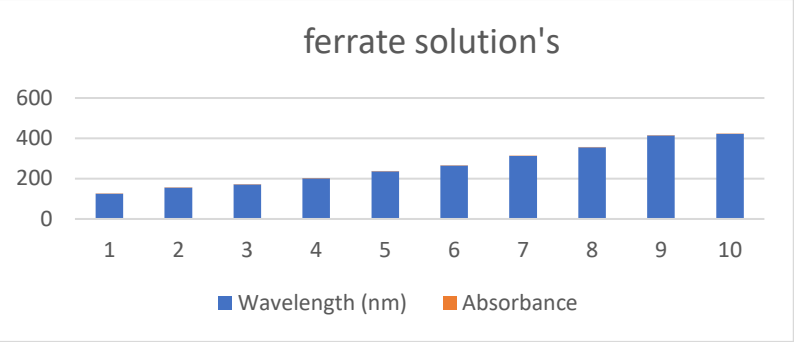

Figure 1: Graphical Representation on ferrate solution's absorbance at 400–700 nm in wavelength

The information displayed includes absorbance measurements at different wavelengths (nm), which shed light on a substance's features related to absorbance throughout the electromagnetic spectrum. The range of absorbance values, which show how much a substance absorbs light at a given wavelength, is 0.1 to 0.8. A higher absorbance number indicates that the substance is able to absorb more light at that specific wavelength. The dataset's analysis shows changes in absorbance at various wavelengths, which may indicate differences in the material's light-interacting properties. Absorbance peaks, like the ones with values of 0.8 at 156 nm and 265 nm, show the wavelengths at which the material absorbs lightest. On the other hand, troughs, such the minimum absorbance of 0.1 at 312 nm, indicate the wavelengths at which the material absorbs light the least. All things considered, this data offers insightful knowledge about the material's optical characteristics, which may have consequences for spectroscopy, materials research, and chemical analysis.

3.3 Ferrate stability test

Using a UV-Vis spectrophotometer, the absorbance of ferrate solution was measured for ten days in order to determine the ferrate stability test. This stability test is used to evaluate the stability and efficacy of ferrate as an oxidant following a predetermined amount of storage time. The data reveal that the ferrate concentration decreased from the first to the tenth day, as depicted in Figure 2. In addition, ferrates decompose, which is visibly identified by variations in the solution's hue. The solution's initial hue is blackish purple, but it quickly turns brownish, signifying that the ferrate has broken down and the solution has turned colorless as a result of the deposition at the bottom of the glass.

These discoveries recommend that after a given measure of time away, ferrate has low oxidative soundness. Since ferrate has solid oxidizing qualities, it has little dependability, which makes it simpler to oxidize other synthetic species in the general climate. Ferrate quickly diminishes to Fe(III) or the insoluble final result (Fe(OH)3) in light of the fact that it is unsound in arrangement. A positive Eocell esteem shows that ferrate separates unexpectedly in water, which delivers the ferrate in the arrangement temperamental.

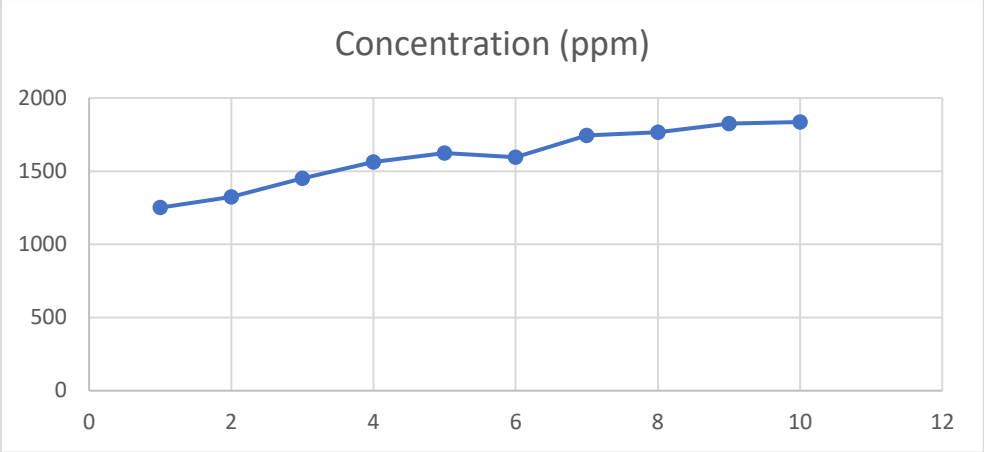

Figure 2: A graph showing the decline in ferrate solution concentration

The dataset offers information on the temporal evolution of a chemical by recording concentrations (ppm) across time (days). The concentration measurements show variations in the substance's concentration throughout the course of the observation period, ranging from 1251 ppm on the first day to 1836 ppm on the tenth. A general tendency of increasing concentration over time is revealed by data analysis, indicating a progressive accumulation or manufacture of the drug. It seems that the rate at which concentration changes varies, with certain days showing larger rises than others. For example, there is a significant concentration increase that occurs between days 3 and 4, rising from 1451 ppm to 1562 ppm. On the other hand, there are times when development is slower or more stable, as seen by the relatively small concentration variations between some days in a row. All in all, this dataset offers insightful data for comprehending the dynamics of substance concentration over time, which may have consequences for disciplines like process optimization, chemical kinetics, and environmental monitoring.

3.4 Determination of optimum pH degradation

Figure 3 illustrates that the maximum proportion of degradation, or 61.6%, happened at pH 8. In contrast, the percentages of degradation for pH 7 and pH 9–11. An essential part of dye degradation is played by ferrate speciation in a number of pH ranges. Ferrates solution contains the species H3FeO4 +, H2FeO4, and HFeO4 - in the acidic environment. The ferrate species involved in neutral conditions are HFeO4- and FeO4-, with HFeO4- species being more prominent; under alkaline solution conditions, on the other hand, the ferrate has FeO4 2- species. A kind of iron monoprotonated species known as HFeO4-has an oxidation capability that is three to five times faster than the dose of FeO4-2 in an aqueous solution.

Table 2: Table showing the ideal pH at which ferrates can degrade Remazol Black B at different pH levels using a 5:1 molar ratio, 60 minutes of contact, and an 8 mL total volume

PH	Degradation (%)
1	57%
2	61%
3	63%
4	65%
5	66%
6	71%

7	75%
8	78%
9	81%
10	86%

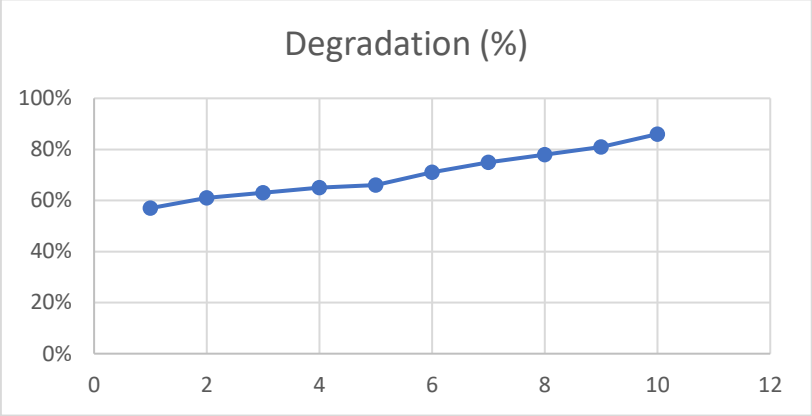

Figure 3: Graph showing the ideal pH at which ferrates can degrade Remazol Black B at different pH levels using a 5:1 molar ratio, 60 minutes of contact, and an 8 mL total volume

The presented dataset shows a substance's percentage of degradation over a given amount of time at various pH values. The degradation percentages show how much the material deteriorates or breaks down at different pH levels; they range from 57% at pH 1 to 86% at pH 10. A consistent pattern of rising degradation percentage with higher pH values is revealed by data analysis. This implies that when the pH of the substance's surroundings increases to an alkaline level, the chemical is more prone to destruction. As pH levels rise, the pace of degradation quickens and the percentage of degradation increases proportionately with each subsequent pH increase. Remarkably, the degradation percentage increases from 71% to 75% between pH levels 6 and 7, marking the largest deterioration leap. This implies that there is a crucial point at which a substance becomes noticeably more susceptible to deterioration. All things considered, this dataset offers insightful information on the substance's pH-dependent degrading behavior, information that may be useful in making decisions about how to handle, store, and mitigate its effects on the environment [21-49].

3.5 Finding the ideal molar ratio for deterioration

One of the key elements influencing how well colors degrade is ferrate content.

At pH 8, the concentration ratio is optimized utilizing a range of ferrate: dye molar ratios (from 1:1 to 5:1) and a 60-minute reaction duration. Results for the ideal molar ratio are displayed in Figure 5. From a 1:1 to a 5:1 molar ratio, the percentage degradation is. These findings suggest that when ferrate ratio concentration rises, so does the efficiency of ferrate decomposition. At a 5:1 molar ratio, the degradation percentage is at its maximum. We can therefore conclude that the ability to degrade increases with increasing ferrate concentration. These findings support the reference, which claimed that the efficiency of degradation rises as the molar ratio decreases.

Table 3: Table showing the ideal molar ratio for ferrate to break down Remazol Black B under different molar ratio conditions, at pH 8, 60 minutes of contact, and 8 mL of total volume.

Molar ratio (ferrate: Remazol Black B)	Degradation %
1:1	20
2:1	25
3:1	31
4:1	42
5:1	51

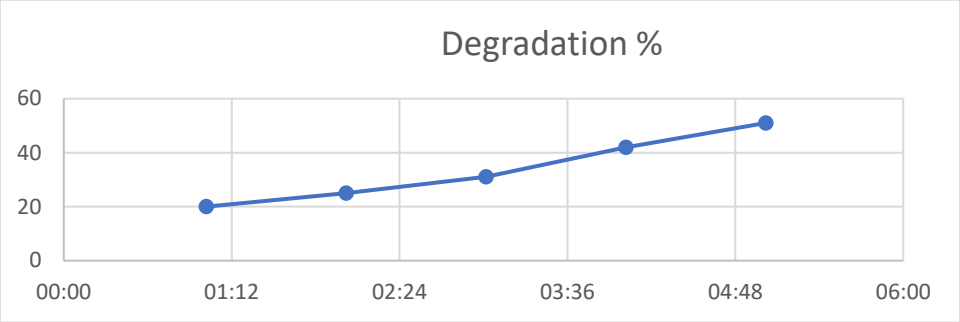

Figure 4: Graph showing the ideal molar ratio for ferrate to break down Remazol Black B under different molar ratio conditions, at pH 8, 60 minutes of contact, and 8 mL of total volume.

The presented dataset provides information on the percentages of dye degradation of Remazol Black B at various molar ratios of ferrate, a possible oxidizing agent. The degradation percentages rise from 20% to 51% in tandem with the molar ratios, which vary from 1:1 to 5:1 (ferrate to Remazol Black B). The molar ratio of ferrate to Remazol Black B and the dye degradation percentage are clearly correlated, according to the data analysis. The degradation percentage rises in proportion to the molar ratio, which indicates increasing ferrate concentrations in relation to the dye. This shows that ferrate breaks down Remazol Black B as an efficient oxidizing agent, with greater concentrations resulting in more substantial deterioration. The trend that has been seen emphasizes how crucial it is to maximize the molar ratio in ferrate-based treatment procedures in order to attain the appropriate degree of dye degradation. Additionally, the data indicates that ferrate exhibits promise as a possible environmentally friendly dye wastewater treatment option, providing chances for the creation of effective and long-lasting remediation plans for effluents from the textile industry.

3.6 Establishing the ideal deterioration time

The best term was found out by molding the ferrate and Remazol Black B colors underneath the best pH and molar proportion (pH 8 and 5:1 molar proportion), then, at that point, changing the length. Tracking down the best second for ferrate to separate Remazol Black B is the objective of this interaction. Figure 5 displays the ferrate data for the optimal deterioration time. According to these findings, the percentage of degradation increases with length of degradation time. After 120 minutes, when the dye's percentage of degradation exceeds 95%, the optimal duration is no longer being determined.

Since adding deterioration time won't significantly alter the outcome, 120 minutes is determined to be the ideal duration. Said another way, the percentage degradation obtained begins at all times.

Table 4: Table showing the ideal pH at different contact durations and a 5:1 molar ratio for the ferrates' breakdown of Remazol Black B dyes over an 8 mL volume.

Time (Minutes)	Degradation (%)
23	31
32	42
41	46
45	51
52	59
59	62
61	67

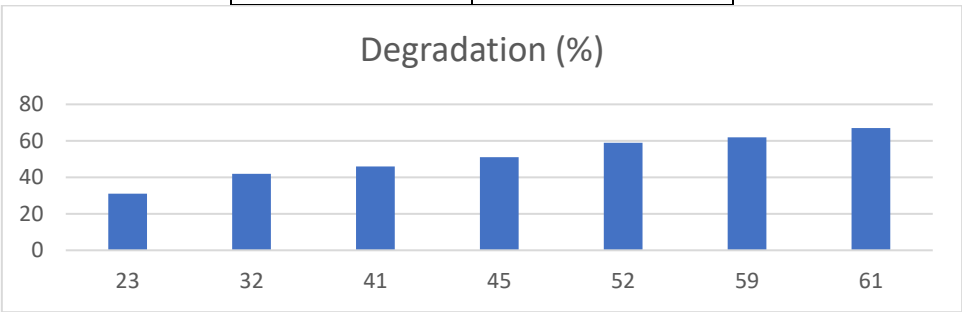

Figure 5: Graph showing the ideal pH at different contact durations and a 5:1 molar ratio for the ferrates' breakdown of Remazol Black B dyes over an 8 mL volume.

The presented dataset provides information on how a material degrades over time, expressed in minutes, along with related percentages of degradation. The degradation percentages show how much the drug has broken down or changed over time, ranging from 31% at 23 minutes to 67% at 61 minutes. A consistent pattern of rising degradation % with longer time intervals is revealed by data analysis. This implies a process of progressive deterioration, in which the substance is continuously broken down or changed during the course of the observation time. Interestingly, there are differences in the proportion of degradation across specific time points, which suggests that the rate of degradation varies. For instance, the deterioration percentage increases significantly from 51% to 59% between 45 and 52 minutes, indicating an increased degradation time. All things considered, this dataset offers insightful information about the kinetics of the degradation process that may be used to guide decisions about treatment protocol optimization or the creation of degradation pathways for the target drug.

4. CONCLUSION

The experimental efforts described in this research in summary, provide noteworthy advancements in the synthesis and kinetics of ferrous sulfate production toward sustainable industrial techniques. The synthesis of ferrate from FeSO4.7H2O was thoroughly explained in the experimental section, along with the tools and supplies needed for the process. with ten days, the stability of the ferrate solution was evaluated, and the results showed that ferrate decomposition caused the concentration to decrease with time. Through experiments looking at pH, molar ratio, and degradation duration, the ideal conditions for Remazol Black B dye breakdown were found. The findings indicated that for maximum dye degradation, pH 8, a molar ratio of 5:1 (ferrate to dye), and a degradation time of 120 minutes were ideal. Ferrate's efficacy in dye degradation was further demonstrated by tests with other oxidizing agents, including KMnO4, H2O2, and K2Cr2O7. Additionally, the effectiveness of dye decomposition

was assessed by COD analysis. Through decreased environmental effect, resource conservation, and improved chemical process efficiency, these findings support the larger objective of promoting sustainable manufacturing practices. For the purpose of developing and implementing sustainable manufacturing processes in the manufacture of ferrous sulfate as well as other industrial sectors, it will be imperative that modeling and optimization research be conducted in the future.

REFERENCES

1. *Abdelfatah, A. M., Fawzy, M., Eltaweil, A. S., & El-Khouly, M. E. (2021). Green synthesis of nano-zero-valent iron using ricinus communis seeds extract: Characterization and application in the treatment of methylene blue-polluted water. ACS omega, 6(39), 25397-25411.*
2. *Aragaw, T. A., Bogale, F. M., & Aragaw, B. A. (2021). Iron-based nanoparticles in wastewater treatment: A review on synthesis methods, applications, and removal mechanisms. Journal of Saudi Chemical Society, 25(8), 101280.*
3. *Bhateria, R., & Singh, R. (2019). A review on nanotechnological application of magnetic iron oxides for heavy metal removal. Journal of Water Process Engineering, 31, 100845.*
4. *Golrizkhatami, F., Taghavi, L., Nasseh, N., & Panahi, H. A. (2023). Synthesis of novel MnFe2O4/BiOI green nanocomposite and its application to photocatalytic degradation of tetracycline hydrochloride:(LC-MS analyses, mechanism, reusability, kinetic, radical agents, mineralization, process capability, and purification of actual pharmaceutical wastewater). Journal of Photochemistry and Photobiology A: Chemistry, 444, 114989.*
5. *Hossain, M. I., Soliman, M. M., El-Naggar, M. E., Sultan, M. Z., Kechi, A., Abdelsalam, N. R., ... & Chowdhury, M. (2021). Synthesis and characterization of graphene oxide-ammonium ferric sulfate composite for the removal of dyes from tannery wastewater. Journal of Materials Research and Technology, 12, 1715-1727.*
6. *Jin, X., Liu, Y., Tan, J., Owens, G., & Chen, Z. (2018). Removal of Cr (VI) from aqueous solutions via reduction and absorption by green synthesized iron nanoparticles. Journal of Cleaner Production, 176, 929-936.*
7. *Kanari, N., Menad, N. E., Ostrosi, E., Shallari, S., Diot, F., Allain, E., & Yvon, J. (2018). Thermal behavior of hydrated iron sulfate in various atmospheres. Metals, 8(12), 1084.*
8. *Karavasilis, M., & Tsakiroglou, C. D. (2019). Synthesis of aqueous suspensions of zero-valent iron nanoparticles (nZVI) from plant extracts: experimental study and numerical modeling. Emerging Science Journal, 3(6), 344-360.*
9. *Karimi, P., Javanshir, S., Sayadi, M. H., & Arabyarmohammadi, H. (2019). Arsenic removal from mining effluents using plant-mediated, green-synthesized iron nanoparticles. Processes, 7(10), 759.*
10. *Katibi, K. K., Yunos, K. F., Man, H. C., Aris, A. Z., Mohd Nor, M. Z., & Azis, R. S. (2021). An insight into a sustainable removal of bisphenol a from aqueous solution by novel palm kernel shell magnetically induced biochar: synthesis, characterization, kinetic, and thermodynamic studies. Polymers, 13(21), 3781.*
11. *Mahmoud, M. E., Saleh, M. M., Zaki, M. M., & Nabil, G. M. (2020). A sustainable nanocomposite for removal of heavy metals from water based on crosslinked sodium alginate with iron oxide waste material from steel industry. Journal of Environmental Chemical Engineering, 8(4), 104015.*

12. *Mohammad Ilias, M. K., Hossain, M. S., Ngteni, R., Al-Gheethi, A., Ahmad, H., Omar, F. M., ... & Pandey, S. (2021). Environmental remediation potential of ferrous sulfate waste as an eco-friendly coagulant for the removal of NH3-N and COD from the rubber processing effluent. International Journal of Environmental Research and Public Health, 18(23), 12427.*
13. *Munagapati, V. S., Wen, H. Y., Gollakota, A. R., Wen, J. C., Shu, C. M., Lin, K. Y. A., ... & Zyryanov, G. V. (2023). Enhanced removal of anionic Methyl orange azo dye by an iron oxide (Fe3O4) loaded lotus leaf powder (LLP@ Fe3O4) composite: Synthesis, characterization, kinetics, isotherms, and thermodynamic perspectives. Inorganic Chemistry Communications, 151, 110625.*
14. *Ngteni, R., Hossain, M. S., Ab Kadir, M. O., Asis, A. J., & Tajudin, Z. (2020). Kinetics and isotherm modeling for the treatment of rubber processing effluent using iron (II) sulphate waste as a coagulant. Water, 12(6), 1747.*
15. *Okpalaeke, K. E., Ibrahim, T. H., Latinwo, L. M., & Betiku, E. (2020). Mathematical modeling and optimization studies by Artificial neural network, genetic algorithm and response surface methodology: a case of ferric sulfate–catalyzed esterification of Neem (Azadirachta indica) seed oil. Frontiers in Energy Research, 8, 614621.*
16. *Qu, J., Liu, Y., Cheng, L., Jiang, Z., Zhang, G., Deng, F., ... & Zhang, Y. (2021). Green synthesis of hydrophilic activated carbon supported sulfide nZVI for enhanced Pb (II) scavenging from water: Characterization, kinetics, isotherms and mechanisms. Journal of Hazardous Materials, 403, 123607.*
17. *Sanjith, U., Choong, W. K., Sivakumar, R., Fauzi, M. N. A., & Rezan, S. A. (2019). Kinetic modelling of oxidation of metallic iron to iron sulfate from iron-titanium oxycarbonitride composite. Materials Today: Proceedings, 17, 525-533.*
18. *Vilardi, G., Rodríguez-Rodríguez, J., Ochando-Pulido, J. M., Verdone, N., Martinez-Ferez, A., & Di Palma, L. (2018). Large Laboratory-Plant application for the treatment of a Tannery wastewater by Fenton oxidation: Fe (II) and nZVI catalysts comparison and kinetic modelling. Process Safety and Environmental Protection, 117, 629-638.*
19. *Wang, Z., Li, H., Zhou, W., Lee, J., Liu, Z., An, Z., ... & Zhou, X. (2022). Ferrous sulfate-loaded hydrogel cures Staphylococcus aureus infection via facilitating a ferroptosis-like bacterial cell death in a mouse keratitis model. Biomaterials, 290, 121842.*
20. *Zhang, J., Yan, Y., Wang, X., Cui, Y., Zhang, Z., Wang, S., ... & Chen, W. (2023). Bridging multiscale interfaces for developing ionically conductive high-voltage iron sulfate-containing sodium-based battery positive electrodes. Nature Communications, 14(1), 3701.*
21. *Mandal S, Vishvakarma P. Nanoemulgel: A Smarter Topical Lipidic Emulsion-based Nanocarrier. Indian J of Pharmaceutical Education and Research. 2023;57(3s):s481-s498.*
22. *Mandal S, Jaiswal DV, Shiva K. A review on marketed Carica papaya leaf extract (CPLE) supplements for the treatment of dengue fever with thrombocytopenia and its drawback. International Journal of Pharmaceutical Research. 2020 Jul;12(3).*
23. *Bhandari S, Chauhan B, Gupta N, et al. Translational Implications of Neuronal Dopamine D3 Receptors for Preclinical Research and Cns Disorders. African J Biol Sci (South Africa). 2024;6(8):128-140. doi:10.33472/AFJBS.6.8.2024.128-140*
24. *Tripathi A, Gupta N, Chauhan B, et al. Investigation of the structural and functional properties of starch-g-poly (acrylic acid) hydrogels reinforced with cellulose nanofibers for*

cu2+ ion adsorption. African J Biol Sci (South Africa). 2024;6(8): 144-153, doi:10.33472/AFJBS.6.8.2024.141-153

25. *Mandal S, Bhumika K, Kumar M, Hak J, Vishvakarma P, Sharma UK. A Novel Approach on Micro Sponges Drug Delivery System: Method of Preparations, Application, and its Future Prospective. Indian J of Pharmaceutical Education and Research. 2024;58(1):45-63.*
26. *Mishra, N., Alagusundaram, M., Sinha, A., Jain, A. V., Kenia, H., Mandal, S., & Sharma, M. (2024). Analytical Method, Development and Validation for Evaluating Repaglinide Efficacy in Type Ii Diabetes Mellitus Management: a Pharmaceutical Perspective. Community Practitioner, 21(2), 29–37. https://doi.org/10.5281/zenodo.10642768*
27. *Singh, M., Aparna, T. N., Vasanthi, S., Mandal, S., Nemade, L. S., Bali, S., & Kar, N. R. (2024). Enhancement and Evaluation of Soursop (Annona Muricata L.) Leaf Extract in Nanoemulgel: a Comprehensive Study Investigating Its Optimized Formulation and Anti-Acne Potential Against Propionibacterium Acnes, Staphylococcus Aureus, and Staphylococcus Epidermidis Bacteria. Community Practitioner, 21(1), 102–115. https://doi.org/10.5281/zenodo.10570746*
28. *Khalilullah, H., Balan, P., Jain, A. V., & Mandal, S. (n.d.). Eupatorium Rebaudianum Bertoni (Stevia): Investigating Its Anti-Inflammatory Potential Via Cyclooxygenase and Lipooxygenase Enzyme Inhibition - A Comprehensive Molecular Docking And ADMET. Community Practitioner, 21(03), 118–128. https://doi.org/10.5281/zenodo.10811642*
29. *Mandal, S. Vishvakarma, P. Pande M.S., Gentamicin Sulphate Based Ophthalmic Nanoemulgel: Formulation and Evaluation, Unravelling A Paradigm Shift in Novel Pharmaceutical Delivery Systems. Community Practitioner, 21(03), 173-211. https://doi.org/10.5281/zenodo.10811540*
30. *Mandal, S., Tyagi, P., Jain, A. V., & Yadav, P. (n.d.). Advanced Formulation and Comprehensive Pharmacological Evaluation of a Novel Topical Drug Delivery System for the Management and Therapeutic Intervention of Tinea Cruris (Jock Itch). Journal of Nursing, 71(03). https://doi.org/10.5281/zenodo.10811676*
31. *Mishra, N., Alagusundaram, M., Sinha, A., Jain, A. V., Kenia, H., Mandal, S., & Sharma, M. (2024). Analytical Method, Development and Validation for Evaluating Repaglinide Efficacy in Type Ii Diabetes Mellitus Management: a Pharmaceutical Perspective. Community Practitioner, 21(2), 29–37. https://doi.org/10.5281/zenodo.10642768*
32. *Singh, M., Aparna, T. N., Vasanthi, S., Mandal, S., Nemade, L. S., Bali, S., & Kar, N. R. (2024). Enhancement and Evaluation of Soursop (Annona Muricata L.) Leaf Extract in Nanoemulgel: a Comprehensive Study Investigating Its Optimized Formulation and Anti-Acne Potential Against Propionibacterium Acnes, Staphylococcus Aureus, and Staphylococcus Epidermidis Bacteria. Community Practitioner, 21(1), 102–115. https://doi.org/10.5281/zenodo.10570746*
33. *Gupta, N., Negi, P., Joshi, N., Gadipelli, P., Bhumika, K., Aijaz, M., Singhal, P. K., Shami, M., Gupta, A., & Mandal, S. (2024). Assessment of Immunomodulatory Activity in Swiss Albino Rats Utilizing a Poly-Herbal Formulation: A Comprehensive Study on Immunological Response Modulation. Community Practitioner, 21(3), 553–571. https://doi.org/10.5281/zenodo.10963801*

34. *Mandal S, Vishvakarma P, Bhumika K. Developments in Emerging Topical Drug Delivery Systems for Ocular Disorders. Curr Drug Res Rev. 2023 Dec 29. doi: 10.2174/0125899775266634231213044704. Epub ahead of print. PMID: 38158868.*
35. *Abdul Rasheed. A. R, K. Sowmiya, S. N., & Suraj Mandal, Surya Pratap Singh, Habibullah Khallullah, N. P. and D. K. E. (2024). In Silico Docking Analysis of Phytochemical Constituents from Traditional Medicinal Plants: Unveiling Potential Anxiolytic Activity Against Gaba, Community Practitioner, 21(04), 1322–1337. https://doi.org/10.5281/zenodo.11076471*
36. *Pal N, Mandal S, Shiva K, Kumar B. Pharmacognostical, Phytochemical and Pharmacological Evaluation of Mallotus philippensis. Journal of Drug Delivery and Therapeutics. 2022 Sep 20;12(5):175-81.*
37. *Singh A, Mandal S. Ajwain (Trachyspermum ammi Linn): A review on Tremendous Herbal Plant with Various Pharmacological Activity. International Journal of Recent Advances in Multidisciplinary Topics. 2021 Jun 9;2(6):36-8.*
38. *Mandal S, Jaiswal V, Sagar MK, Kumar S. Formulation and evaluation of carica papaya nanoemulsion for treatment of dengue and thrombocytopenia. Plant Arch. 2021;21:1345-54.*
39. *Mandal S, Shiva K, Kumar KP, Goel S, Patel RK, Sharma S, Chaudhary R, Bhati A, Pal N, Dixit AK. Ocular drug delivery system (ODDS): Exploration the challenges and approaches to improve ODDS. Journal of Pharmaceutical and Biological Sciences. 2021 Jul 1;9(2):88-94.*
40. *Shiva K, Mandal S, Kumar S. Formulation and evaluation of topical antifungal gel of fluconazole using aloe vera gel. Int J Sci Res Develop. 2021;1:187-93.*
41. *Ali S, Farooqui NA, Ahmad S, Salman M, Mandal S. Catharanthus roseus (sadabahar): a brief study on medicinal plant having different pharmacological activities. Plant Archives. 2021;21(2):556-9.*
42. *Mandal S, Vishvakarma P, Verma M, Alam MS, Agrawal A, Mishra A. Solanum Nigrum Linn: An Analysis Of The Medicinal Properties Of The Plant. Journal of Pharmaceutical Negative Results. 2023 Jan 1:1595-600.*
43. *Vishvakarma P, Mandal S, Pandey J, Bhatt AK, Banerjee VB, Gupta JK. An Analysis Of The Most Recent Trends In Flavoring Herbal Medicines In Today's Market. Journal of Pharmaceutical Negative Results. 2022 Dec 31:9189-98.*
44. *Mandal S, Vishvakarma P, Mandal S. Future Aspects And Applications Of Nanoemulgel Formulation For Topical Lipophilic Drug Delivery. European Journal of Molecular & Clinical Medicine.;10(01):2023.*
45. *Chawla A, Mandal S, Vishvakarma P, Nile NP, Lokhande VN, Kakad VK, Chawla A. Ultra-Performance Liquid Chromatography (Uplc).*
46. *Mandal S, Raju D, Namdeo P, Patel A, Bhatt AK, Gupta JK, Haneef M, Vishvakarma P, Sharma UK. Development, characterization, and evaluation of rosa alba l extract-loaded phytosomes.*
47. *Mandal S, Goel S, Saxena M, Gupta P, Kumari J, Kumar P, Kumar M, Kumar R, Shiva K. Screening of catharanthus roseus stem extract for anti-ulcer potential in wistar rat.*
48. *Shiva K, Kaushik A, Irshad M, Sharma G, Mandal S. Evaluation and preparation: herbal gel containing thuja occidentalis and curcuma longa extracts.*

49. *Vishvakarma P, Kumari R, Vanmathi SM, Korni RD, Bhattacharya V, Jesudasan RE, Mandal S. Oral Delivery of Peptide and Protein Therapeutics: Challenges And Strategies. Journal of Experimental Zoology India. 2023 Jul 1;26(2).*